

Communication

Occurrence and Removal of Copper and Aluminum in a Stream Confluence Affected by Acid Mine Drainage

Carolina Rodríguez ¹, Enzo Leiva-Aravena ¹, Jennyfer Serrano ² and Eduardo Leiva ^{1,3,*} 

¹ Departamento de Ingeniería Hidráulica y Ambiental, Pontificia Universidad Católica de Chile, Avenida Vicuña Mackenna 4860, Macul, Santiago 7820436, Chile; cnrodriguez@uc.cl (C.R.); erleiva@uc.cl (E.L.-A.)

² Escuela de Biotecnología, Universidad Mayor, Camino La Pirámide 5750, Huechuraba, Santiago 8580745, Chile; jennyfer.serrano@umayor.cl

³ Departamento de Química Inorgánica, Facultad de Química, Pontificia Universidad Católica de Chile, Avenida Vicuña Mackenna 4860, Macul, Santiago 7820436, Chile

* Correspondence: ealeiva@uc.cl; Tel.: +56-2-2354-7224

Received: 10 February 2018; Accepted: 6 April 2018; Published: 20 April 2018



Abstract: Acid mine drainage (AMD) is an environmental concern characterized by low pH and high concentrations of dissolved metals and sulfate. Yerba Loca Creek in Santiago, Chile, is an AMD-affected water stream that originates in a glacier and, therefore, has a season-dependent flow. This water course is characterized by low pH (3.75 ± 0.13) and high concentrations of aluminum (2.2–2.6 mg/L) and copper (4.8–6.5 mg/L). A field campaign was carried out to study the geochemical behavior around the confluence of the Yerba Loca Creek with the San Francisco River, which has a neutral pH and low concentration of dissolved metals. The results show that the geochemical parameters after the confluence are very similar to those registered for the Yerba Loca Creek, due to its great flow in relation to the San Francisco River. The pH after the mixing zone was controlled by the geochemical conditions and flow of the Yerba Loca Creek; however, the turbidity decreases and stabilizes downstream. We found that, despite the low impact of pH on the precipitation of aluminum and copper phases due to poor neutralization, the dissolved aluminum and copper concentrations are slightly decreased after the mixing zone by natural microscale removal processes or suspended solids formation. Scanning electron microscopy–energy-dispersive X-ray spectroscopy (SEM–EDX) analysis of suspended solids indicates the presence of various oxides, hydroxy-sulfates and aluminosilicates, which have a great affinity for adsorption and co-precipitation with dissolved metals (i.e., Al and Cu). A pH-neutralization would favor the formation of more minerals and, therefore, the immobilization of the heavy metals found in these waters. These results contribute to a better understanding of the effect of the confluence of water courses related to pollution by AMD. It is possible that the seasonal variation of the flows has an impact on the composition of water and minerals formed.

Keywords: acid mine drainage; low pH; metals solubility; confluence

1. Introduction

Acid mine drainage (AMD) is a major problem all over the world. AMD is produced when sulfide-bearing material, from mine sites or natural sources, is exposed to water and oxygen [1,2]. The main problem caused by AMD is pollution due to low pH, high concentrations of dissolved metals (i.e., iron, aluminum, copper, lead, zinc and silver, among others), metalloids (e.g., arsenic) and sulfate [3]. The level of environmental impact of AMD is dependent on its composition (i.e., which dissolved metals are present) and its pH values, in turn, depend on the geology of the AMD source [3].

Yerba Loca Creek is a natural water course located in Santiago, Chile, and is affected by AMD. The creek basin extends for 16 km from the La Paloma glacier to its confluence with the San Francisco

River (pH ~7.2) [4]. At high elevations of the Yerba Loca Basin, there is a large deposit of copper porphyry, which have long influenced the surface water quality of the area, particularly in terms of pH, sulfate content and mineral concentrations [5]. In particular, in the Yerba Loca Creek acidic conditions and metal content, mainly copper (Cu) and aluminum (Al) [6], have a substantial impact on the vegetation of the area since these waters are highly toxic for most plant species [5]. Furthermore, the presence of Cu in excessive concentrations is harmful to a variety of living organisms such as microorganisms, fish and humans [7]. In the environment, Cu is commonly presented as a divalent cation and is generally more mobile in acidic conditions, while at pH above 7, it tends to form minerals like Cu carbonates and hydroxyl-carbonates [8,9]. Al is the third most abundant element in the Earth's crust and is commonly present as Al oxide and Al silicate [10,11]. At pH less than 6, Al can be leached from the soil and sediments in the water [10], but the solubility increases when pH is less than 4.5 [12]. In addition, high Al concentrations, low pH and high levels of sulfate generate toxicity in the aquatic environment, which can be fatal for animal and plant life [13].

Several studies have been carried out about the effects of the confluence of water courses related to pollution by AMD. The Azufre River–Caracarani River Confluence (Chile) presents a change in particle sizes and a decrease in As concentration after the confluent point [14]. Agrio River–Odiel River Confluence (Spain) shows a strong seasonal variation in water composition [15]. For its part, Cement Creek–Animas River Confluence (USA) is a mixing zone of two water courses with acidic pH (Cement Creek) and neutral pH (Animas River). The complete mixing results in a circumneutral pH and metals in solution exhibit transformations to colloidal forms [16]. The mixing zone receiving acid drainage is a reactive zone where changes in pH and the chemical environment promotes the formation and precipitation of minerals [14]. Metal partitioning between the solid phase and solution can be modified along the flow path by changes in pH, redox and biotic factors downstream of the mixing zone [17,18]. The description and quantification of non-conservative processes that control the fate of metals in natural environments are critical for the development of environmental remediation in systems affected by acid mine drainage [19,20]. Reactive confluences form when acid drainage discharges into a circumneutral river are an opportunity to study how the geochemical processes in the solid/liquid interface modify the aqueous/solid partitioning of heavy metals.

In this study, on-site measurements and water samples analysis were carried out to determine the geochemical behavior in the Yerba Loca Creek–San Francisco River confluence in a radius of 50 m around the confluence point. The objective of this study was to determine the effect of the confluence on pH and the fate of Cu and Al and the formation of minerals. This study will help to improve our knowledge about the processes that control the transport, removal and environmental fate of Al and Cu in acid mine drainage waters and thus contribute to the development of new alternatives for enhanced natural attenuation of these pollutants.

2. Materials and Methods

2.1. Study Site

The research was carried out in December 2017 at the Yerba Loca Creek–San Francisco River confluence located outside of the Yerba Loca Nature Sanctuary (33°20'42.23" S; 70°21'50.77" W) in the pre-mountain range zone of Santiago, Chile.

Yerba Loca Creek has an average flow of 1.35 m³/s in summer months, due to the melting of the glacier, and an average flow of 0.33 m³/s in winter months. On the other hand, San Francisco river before the junction has a stable flow during the year, with an average of 0.22 m³/s [21]. The flow ratio is an important parameter because it can vary seasonally and, in this way, the effect of the confluence varies depending on the mixing proportion [14].

2.2. Sampling and On-Site Measurements

A total of 19 water samples were collected from the study site. A sample was taken from the confluence point which was defined as the zero point. Additionally, six sampling points were defined for both the San Francisco River and the Yerba Loca Creek before the confluence and six samples for the San Francisco River after the confluence. In all cases, sampling points were located at 5 m, 10 m, 20 m, 30 m, 40 m and 50 m away from the confluence point (Figure 1a). On-site measurements were performed at these points, including pH (PHC301, HACH, Loveland, CO, USA), electrical conductivity (EC) (CDC401, HACH), dissolved oxygen (DO) (LDO101, HACH), and temperature (PHC301, HACH) (Hq40d Multi, HACH, Loveland, CO, USA) measurements.

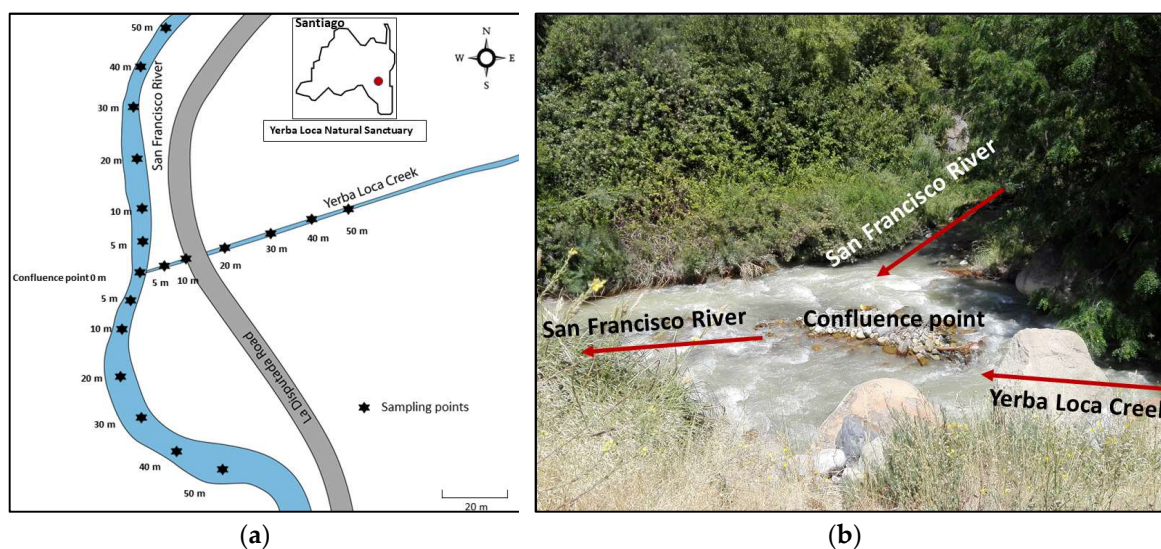


Figure 1. (a) Schematic representation of the study site at the confluence of the San Francisco River and Yerba Loca Creek, in the north-east of Santiago; (b) Photograph of the confluence point of both water courses.

The water samples were collected in 1000 mL high-density polyethylene (HDPE) bottles and stored in darkness at 4 °C until analysis. For anion and cation measurements, samples were filtered at 0.22 μm . In the case of cation measurements, the samples were also acidified with HNO_3 . For dissolved metals analysis, water samples were filtered at 0.45 μm and acidified with HNO_3 . In addition, for soluble chemical oxygen demand (sCOD) measurement, water samples were filtered at 0.45 μm and acidified with H_2SO_4 . Additionally, the turbidity of the water samples was measured using a Hanna HI 98703 turbidimeter (Hanna Instruments Inc., Woonsocket, RI, USA).

2.3. Geochemical Analysis

Anion and cation measurements were made by ion chromatography (IC) (882 compact IC plus, Metrohm, Herisau, Switzerland) and total dissolved metal concentrations were carried out by a total reflection X-ray fluorescence (TXRF) spectrometer "S2 PICOFOX" (Bruker AXS Microanalysis, Berlin, Germany). Additionally, sCOD was determined colorimetrically in a HACH spectrophotometer DR/2010 with the reactor digestion method (USEPA Method 8000) [22].

2.4. Scanning Electron Microscopy (SEM)

Total suspended solids (TSS) obtained by 0.22- μm filtration were analyzed by scanning electron microscopy (JSM-IT300LV; JEOL Ltd., Tokyo, Japan) coupled with energy-dispersive X-ray spectroscopy (Oxford Instruments, HighWycombe, UK) (SEM-EDX). Prior to the observation, these solids were lyophilized for 24 h and subsequently coated with gold.

3. Results and Discussion

3.1. Water Parameters

One relevant parameter in water quality is pH since this affects the solubility of metal ions [23]. On-site measurements show a neutral pH in the San Francisco River before the confluence while the Yerba Loca Creek has a pH of 3.75 ± 0.13 before the junction (Figure 2a). After the confluence, the pH remains very similar to the value of the Yerba Loca Creek, with a low increase of 0.2 units. This is expected due to low flow of the San Francisco River (pH ~ 7.2) compared to the Yerba Loca flow, despite the noticeable difference between pre-confluence pH values. Interestingly, iron (Fe) and Al phases such as schwertmannite ($\text{Fe}_8\text{O}_8(\text{OH})_x\text{SO}_y \cdot n\text{H}_2\text{O}$; where $8 - x = y$ and $y = [1-1.75]$), and hydrobasaluminite ($\text{Al}_4(\text{SO}_4)(\text{OH})_{10} \cdot [12-36]\text{H}_2\text{O}$) can precipitate in the pH range between [2.8–4.2] and [4–4.5], respectively [24]. Thus, pH behavior after confluence can influence the precipitation and removal of metals from the aqueous phase. In addition, PHREEQC (acronym of pH-Redox-Equilibrium-C+ language program) speciation models show that small variations in pH can allow the formation of certain minerals (Appendix A). The relevance of these precipitated phases lies not only in the control of the solubility of Al and Fe, but also in the impact on the removal of sulfate and other metals such as Cu and Zn by adsorption/coprecipitation processes.

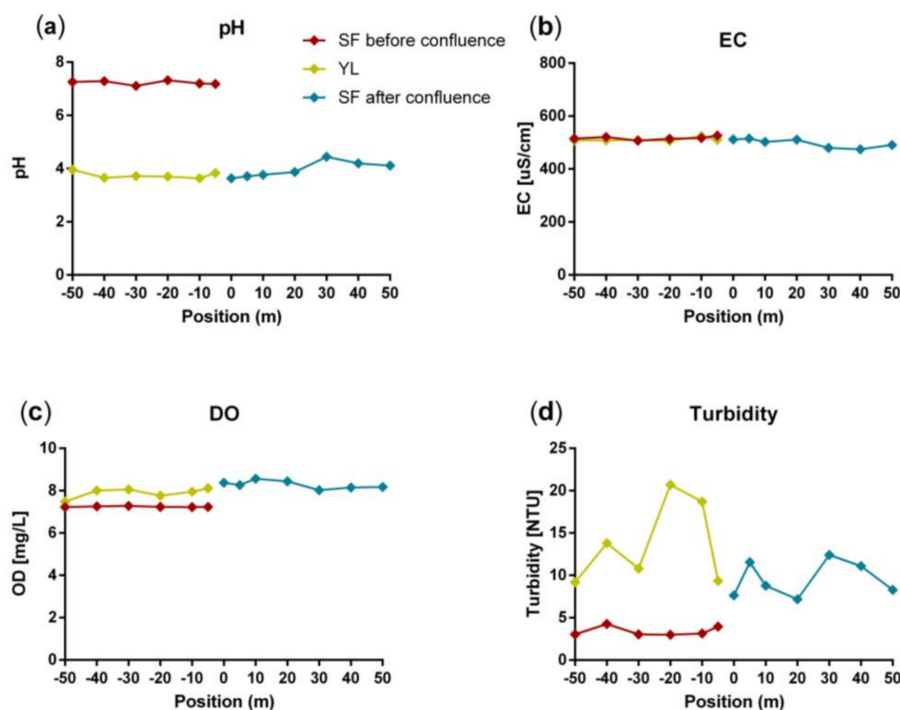


Figure 2. Water parameters of the study site: (a) pH; (b) Electric conductivity; and (c) Dissolved oxygen correspond to on-site measurements; while (d) Turbidity was measured in the laboratory. Symbology is related to the San Francisco River (SF) before the confluence and after the confluence, and the Yerba Loca Creek (YL).

The electrical conductivity of both water courses is similar before and after the confluence (Figure 2b). However, historical data from the Yerba Loca Creek before the confluence report that EC reaches values upper than 360 mS/cm in some months of the year. In the same way as EC, the DO measurements show a similar behavior in all the sampled points (Figure 2c). DO values close to 8 mg/L indicate that there is no contamination by organic matter nor an important metabolic activity because of organic matter degradation or eutrophication [25]. The sCOD data confirms this, reporting values in a range of 0–124 mg/L.

Regarding turbidity measurements, Yerba Loca Creek presents a much greater value than the San Francisco River before the confluence, causing an intermediate turbidity value after the mix of the two courses (Figure 2d). Furthermore, turbidity is greater than 3.0 nephelometric turbidity units (NTU) for all sampling points, with a peak of 20.7 NTU in Yerba Loca Creek, 20 m before confluence. Although these values exceed the Chilean normative for drinking waters (<2 NTU) [26], they belong to a typical range of healthy bodies of water. Figure 2d shows that changes in turbidity are less marked downstream from the confluence, showing a peak of increase at 5 m and 30 m after the confluence. The turbidity was lower than in the Yerba Loca Creek before the confluence, which could indicate local reactive phenomena in the mixing zone that cause changes in the solid/liquid interface at microscale level and thus promote the formation of suspended solids enriched in heavy metals. These conditions may be independent of the pH effect. Besides, the conditions before and after the confluence are similar, so external effects such as wind should not have a greater impact on turbidity.

3.2. Anions and Cations

Anion and cation concentrations measured at different sampling points (Table 1) reveal a high amount of sulfate at all the points, exceeding the drinking water standard of 500 mg/L in some cases [26]. High concentrations of sulfate are characteristic of AMD and the oxidation of metal sulfides [1]. These concentrations limit the use of water for various purposes (e.g., drinking water and irrigation water) [26,27].

Table 1. Concentration of anions and cations in water samples.

Sample		Anions (ppm ¹)			Cations (ppm ¹)			
		Sulfate	Chloride	Nitrate	Sodium	Potassium	Calcium	Magnesium
San Francisco River before confluence	5 m	184.1	43.4	1.9	25.0	3.6	69.1	13.4
	10 m	293.2	79.9	3.2	25.1	3.6	72.0	13.9
	20 m	225.1	52.6	2.9	24.7	5.4	68.5	13.6
	30 m	326.1	87.4	3.9	25.1	6.5	69.5	13.3
	40 m	304.9	85.7	4.5	25.2	16.6	70.1	13.5
	50 m	311.2	85.0	4.5	25.3	13.2	68.4	13.8
Yerba Loca Creek	5 m	351.9	4.5	6.0	4.2	2.8	71.7	9.3
	10 m	405.5	4.9	3.1	4.2	2.4	72.9	9.2
	20 m	503.0	4.5	1.7	4.1	6.2	71.6	9.4
	30 m	297.7	2.9	1.6	4.3	1.7	70.6	9.3
	40 m	507.2	4.5	2.1	4.2	2.4	69.6	9.2
	50 m	341.8	3.4	1.3	4.1	2.0	71.4	9.3
San Francisco River after confluence	0 m	318.6	3.1	1.7	4.0	3.0	70.6	14.0
	5 m	504.7	6.0	2.3	4.2	1.9	72.1	9.6
	10 m	330.7	3.4	1.6	4.2	3.9	73.3	10.3
	20 m	309.6	4.9	1.2	5.3	3.1	71.4	10.6
	30 m	312.4	12.1	2.0	7.7	13.6	69.9	9.9
	40 m	285.7	8.2	1.7	7.5	5.3	74.4	9.9
	50 m	472.0	10.8	2.3	6.4	2.4	71.8	10.1

¹ Parts per million.

Sodium and chloride present a decrease along the San Francisco River from the point of confluence forward, due to the dilution that occurs when both flows are combined. These decreases in sodium and chloride go, on average, from 25.06 ppm to 5.62 ppm and from 72.34 ppm to 6.94 ppm, respectively. Conversely, sulfate concentration increased in San Francisco River after the confluence due to the high concentration of sulfate from the Yerba Loca Creek. On the other hand, all registered cations (i.e., calcium, magnesium and potassium) and nitrate did not present significant variations before and after the confluence. In summary, due to the low flow of the San Francisco River in relation to the Yerba Loca Creek, the anion and cation concentrations after confluence are strongly influenced by the concentrations from the Yerba Loca Creek. However, variations in sulfate concentrations may indicate variations in microscale precipitation/dissolution processes and be influenced by hydrodynamic conditions. Guerra et al. [28]. showed that in a confluence impacted by acid mine drainage the

interaction between chemical and hydrodynamic conditions controls the transport of metals such as Fe, Al and arsenic (As) downstream of reactive confluences.

3.3. Dissolved Metals

Dissolved metals analysis showed four main metals present in the study site: Al, Cu, and manganese (Mn). Concentrations of Fe and Mn are similar between the Yerba Loca Creek and San Francisco River after the confluence (Figure 3), due to the low flow of the San Francisco River in relation to the Yerba Loca Creek. However, a slight removal of dissolved Al and Cu concentrations were observed. The removal is most evident for Cu (Figure 3b). This effect is especially evident for Al and Cu because their concentrations for the San Francisco River before the confluence resulted non-detectable or nearly zero, respectively (Figure 3a,b).

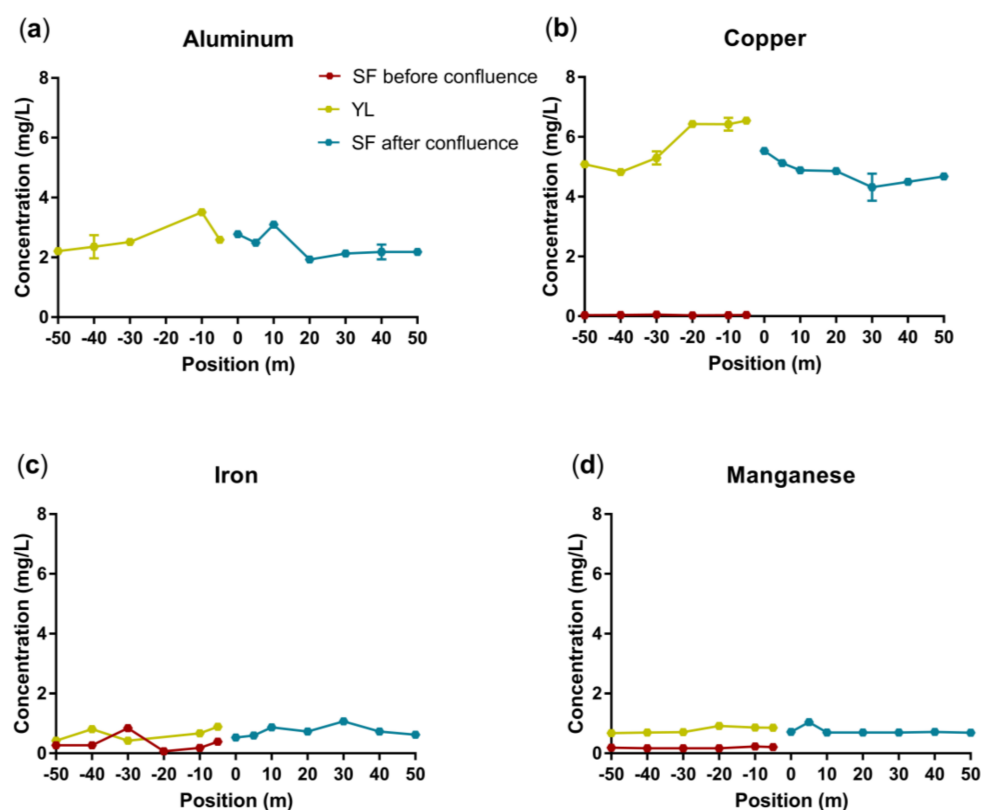


Figure 3. Dissolved concentrations of (a) Aluminum, (b) Copper, (c) Iron and (d) Manganese in the San Francisco River (SF) and Yerba Loca Creek (YL), before and after the confluence. Error bars correspond to the standard deviation of the measurements made in triplicate. In some cases, the error bars are not observed because the standard deviation of the results is very small. Aluminum concentration was not detected in the San Francisco River before the confluence (a).

In the case of Al, since its solubility increases linearly as the pH decreases in the range of neutral to acidic values [10], it is expected that Al is not present in the liquid phase at neutral pH conditions, as occurs in the San Francisco River before the confluence. Regarding Cu concentrations, they are higher than 4 mg/L in the Yerba Loca Creek and San Francisco River after the junction, exceeding the maximum level allowed for drinking water in Chile, corresponding to 2 mg/L [26].

In the case of change in the flow ratio between both flows, for example due to seasonal variation of the flow of the Yerba Loca Creek, a dilution effect could be generated and a consequent impact on the pH and concentration values after the junction. Therefore, as a final consequence, the removal of Al and Cu due to precipitation processes could be generated, as has been done for other confluences [14–16].

Abarca et al. [14] show that after the Azufre River–Caracarani River confluence, particle sizes varied, and the dissolved As concentration decreased. On the other hand, Schemel et al. [16] reported that from the Cement Creek–Animas River confluence, dissolved metals (i.e., Al, Fe, Cu and zinc) exhibited transformations from dissolved to colloidal forms to varying degrees during the mixing process. However, flow data of the Yerba Loca Creek–San Francisco River confluence indicate that changes in the Al and Cu dissolved concentrations are not explained by a dilution effect due to the low flow of the San Francisco River.

Typically, the pH range reported for limiting the precipitation of Al is [4.5–5.0] [29–31]. These pH values are far from the pH value (~3.9) observed after the confluence between the Yerba Loca Creek and San Francisco River, suggesting that the precipitation processes of Al phases are not significant. However, pH values around 4.0 for Al precipitation have been observed in several field studies and laboratory experiments with AMD waters, indicating that the formation of gibbsite ($\text{Al}(\text{OH})_3$) or another Al-hydroxide phase can occur in values close to this pH and promote the removal of Al. Bertsch and Parker [32] suggest that the presence of sulfate ions decreases the pH necessary for Al precipitation, favoring the formation and aggregation of polynuclear Al species increasing the rates of nucleation and precipitation. Therefore, the pH values (Figure 2) and the sulfate concentrations after confluence (411 ± 94 mg/L) suggest that the phases of Al hydroxy-sulfate minerals as basaluminite ($\text{Al}_4(\text{SO}_4)(\text{OH})_{10} \cdot [4-5]\text{H}_2\text{O}$) and hydrobasaluminite ($\text{Al}_4(\text{SO}_4)(\text{OH})_{10} \cdot [12-36]\text{H}_2\text{O}$) could precipitate. Furthermore, it has been observed that with the progressive neutralization of the pH of sulfate-rich acidic waters the formation of Al hydroxy-sulfate minerals is increasingly favored [33]. Carrero et al. [34] reported that basaluminite has a high capacity to retain Cu by precipitation or adsorption, which would explain the Cu removal observed after the confluence. Additionally, hydrogeochemical modeling with PHREEQC shows that at pH upper 4, alunite ($\text{KAl}_3(\text{SO}_4)_2(\text{OH})_6$) could be formed (see Table A2), which confirms the presence of hydroxy-sulfate minerals.

In the case of Fe, the concentration of all sampled points ranges between 0 and 1 mg/L. In other systems, the precipitation of Fe as schwertmannite has been observed at pH values close to 3.5 [35,36]; however, the impact on the removal of dissolved Fe for our system was not sufficiently evident to be certain that this occurs. De Souza Machado et al. [37] indicated that high turbulence can promote the solubility of some metal precipitates, which could explain that there is no dissolved Fe removal after the confluence. Finally, a removal of dissolved Mn species in relation to the Yerba Loca Creek before the confluence (Figure 3d) was not observed.

Other minerals that are typically formed in acid mine drainage systems are Fe and Mn oxides. In both cases, Cu can bind strongly to the surface of oxides formed with these metals [38]. Furthermore, precipitation in natural systems generates initially amorphous minerals, which may have a greater capacity of sorption by affinity with the binding sites to other minerals [39,40]. In particular, it has been demonstrated that Fe oxides and Mn oxides can adsorb other dissolved metals like As, lead, zinc and cadmium, removing them from the aqueous phase [41,42]. Due to the low flow of San Francisco River, a potential removal of the contamination present in the Yerba Loca Creek could be focused on channeling a part of the flow of the river to be treated.

3.4. Scanning Electron Microscopy (SEM)

Images taken by SEM at different magnifications show that suspended solids at sampling points correspond mainly to granules of varied sizes (Figure 4). The morphology and composition of these crystals are typical of natural waters enriched with heavy metals [43].

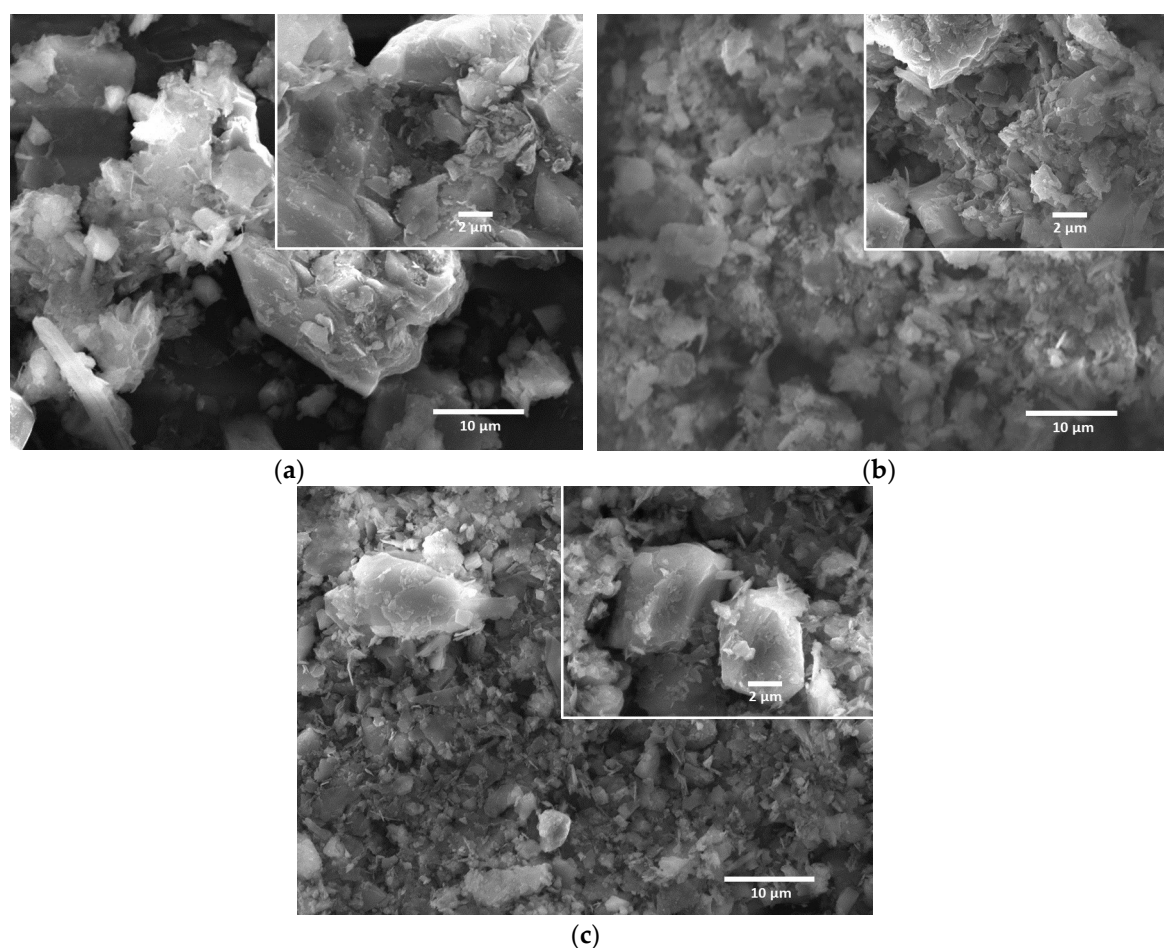


Figure 4. Scanning electron micrographs of total suspended solids obtained from (a) San Francisco River before confluence; (b) Yerba Loca Creek and (c) San Francisco River after confluence.

SEM–EDX analysis was carried out for TSS of three selected points, San Francisco River 10 m before confluence, Yerba Loca Creek 10 m before confluence, and San Francisco River 10 m after confluence. In general, EDX analyses of the three samples show the presence of Al, Cu, Fe and O elements. In addition, suspended solids were analyzed by portable X-ray fluorescence (PXRF), which confirm the presence of the mentioned elements and sulfur (S) in a concentration of approximately 5800 ppm after the confluence point, suggesting the formation of Fe and Al oxyhydroxide-sulfate complexes [44] (Figure 5).

In addition, an important silicon (Si) content is observed. Soils generally contain 5–40% silicon (Si), which is mainly found in the form of SiO_2 and several aluminosilicates [45]. Furthermore, suspended sediment in rivers has an average of 25.4% in Si content [46]. After the confluence, the surface concentrations of Al and Si in TSS reached 7.6 wt % and 31.5 wt %, respectively, suggesting the formation of aluminosilicates (Figure 5c).

Consistent with the analysis of dissolved metals (See Figure 3), the San Francisco River before the confluence has a lower amount of Al in the suspended solids with respect to the other studied points. As mentioned above, in acid waters Al is controlled by the solubility of gibbsite ($\text{Al}(\text{OH})_3$) and kaolinite ($\text{Al}_2\text{Si}_2\text{O}_5(\text{OH})_4$) minerals [47]. However, in the presence of sulfate, these minerals are no longer stable and other less soluble minerals can control the aqueous geochemistry of Al. For this reason, the precipitation of Al hydroxysulfates immobilizes Al and sulfate in acid waters [31,47].

Regarding Cu, this can form more complexes as the pH increases, so it becomes less bioavailable and, therefore, less toxic [48]. According to McBride et al. [49], most of the Cu is complexed above pH

5. Furthermore, dissolved Cu has an affinity for adsorption with aluminosilicates present in natural waters [50]. Therefore, considering the neutral pH of the San Francisco River before the confluence, plus the amounts of Si and O present in its suspended solids, it is expected that Cu content would be found in them. On the other hand, suspended solids of the Yerba Loca Creek and San Francisco River after the confluence, both characterized by low pH conditions, were expected not to have too much Cu in their composition.

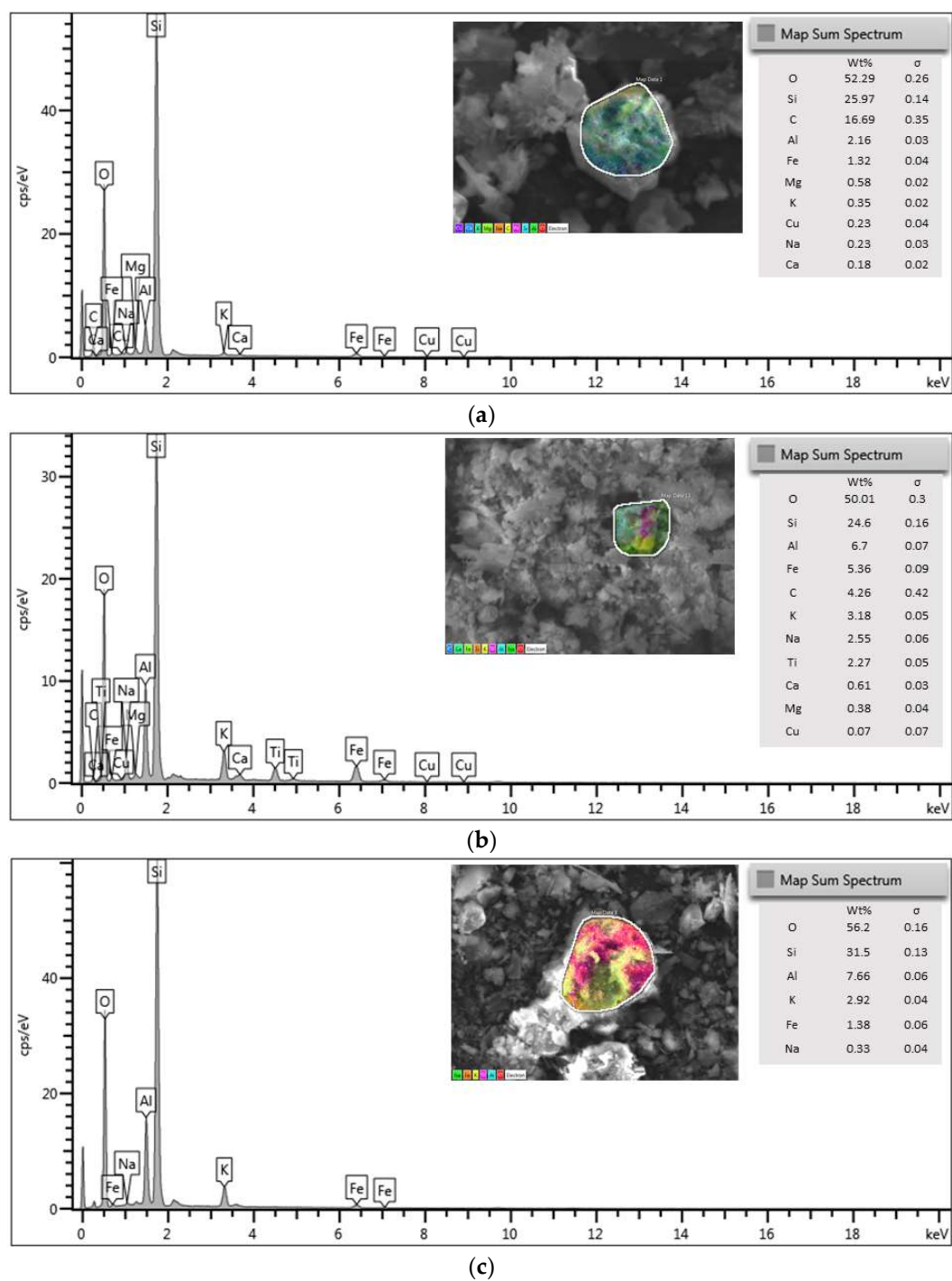


Figure 5. Energy-dispersive X-ray spectra of suspended solids obtained from (a) San Francisco River before confluence; (b) Yerba Loca Creek and (c) San Francisco River after confluence. C, O, Si, and Al are the main elements identified in the samples.

4. Conclusions

The studied confluence site is strongly influenced by the high flow of the Yerba Loca Creek, which is substantially higher than the flow of the San Francisco River in summer. In this way, the water quality of the San Francisco River after the confluence is heavily governed by the geochemical parameters of the Yerba Loca Creek. The main effects that occur in the San Francisco River after the confluence correspond to a pH decrease ($-\Delta 3.48$) and high increases in Al and Cu concentrations. After the confluence, a slight removal of dissolved Al and Cu concentrations was observed, which could be explained by an effect of pH and a high concentration of sulfate. These conditions can promote the formation of Al hydroxy-sulfate minerals such as basaluminite and hydrobasaluminite, which have the potential to retain Cu by adsorption/coprecipitation processes. Moreover, analysis of suspended solids by SEM-EDS indicates the presence of various oxides, hydroxy-sulfates and aluminosilicates, which have a great affinity for adsorption and co-precipitation with metals dissolved in water. It is expected that, with a view to a potential remediation of this site, a pH-neutralization mechanism could favor the formation of more minerals and, therefore, the immobilization of the heavy metals found in these waters.

It is necessary to carry out studies from other perspectives, such as those studying the possible impact of seasonal variation of the flow of the Yerba Loca Creek on the geochemical behavior of the confluence. In addition, it is essential to study the San Francisco River downstream at a greater distance in order to analyze the water composition and the possible precipitation of minerals due to changes in the environmental conditions.

Acknowledgments: This research was funded by PIA-UC Eduardo Leiva/DDA-VRA.

Author Contributions: The manuscript was written by Carolina Rodríguez, but all the authors contributed to its preparation and review. Experiments were performed by Carolina Rodríguez. Data analyses were carried out by Carolina Rodríguez in discussion with Eduardo Leiva, Enzo Leiva-Aravena and Jennyfer Serrano. All the authors participated in the field campaign.

Conflicts of Interest: The authors declare no conflict of interest.

Appendix A. Distribution of Aqueous Species in San Francisco River Modeled by PHREEQC

Table A1. Saturation state in Yerba Loca Creek–San Francisco River confluence (pH = 3.63).

Phase		Saturation Index (SI)	log Ion Activity Product (IAP)	log Equilibrium Constant (KT) at 13.1°C
Aluminum hydroxide	Al(OH) ₃ (a)	−5.61	5.99	11.61
Alunite	KAl ₃ (SO ₄) ₂ (OH) ₆	−2.66	−2.53	0.13
Anhydrite	CaSO ₄	−1.41	−5.74	−4.33
Iron hydroxide	Fe(OH) ₃ (a)	−8.58	−3.69	4.89
Gibbsite	Al(OH) ₃	−2.81	5.99	8.80
Goethite	FeOOH	−3.13	−3.69	−0.56
Gypsum	CaSO ₄ ·2H ₂ O	−1.16	−5.74	−4.59
H ₂ (g)	H ₂	−15.30	−18.40	−3.10
H ₂ O(g)	H ₂ O	−1.83	−0.00	1.83
Halite	NaCl	−9.46	−7.91	1.55
Hausmannite	Mn ₃ O ₄	−42.42	21.68	64.10
Hematite	Fe ₂ O ₃	−4.31	−7.37	−3.07
Jarosite-K	KFe(SO ₄) ₂ (OH) ₆	−23.32	−31.58	−8.26
Manganite	MnOOH	−15.57	9.77	25.34
Melanterite	FeSO ₄ ·7H ₂ O	−5.63	−7.99	−2.37
O ₂ (g)	O ₂	−56.87	−59.67	−2.80
Pyrochroite	Mn(OH) ₂	−13.06	2.14	15.20
Pyrolusite	MnO ₂ ·H ₂ O	−25.96	17.40	43.36

Table A2. Saturation state in San Francisco River 30 m after the confluence point (pH = 4.44).

Phase		Saturation Index (SI)	log Ion Activity Product (IAP)	log Equilibrium Constant (KT) at 14.7°C
Aluminum hydroxide	Al(OH) ₃ (a)	−3.20	8.29	11.50
Alunite	KAl ₃ (SO ₄) ₂ (OH) ₆	2.67	2.59	−0.08
Anhydrite	CaSO ₄	−1.41	−5.75	−4.34
Iron hydroxide	Fe(OH) ₃ (a)	−5.80	−0.91	4.89
Gibbsite	Al(OH) ₃	−0.42	8.29	8.71
Goethite	FeOOH	−0.29	−0.91	−0.62
Gypsum	CaSO ₄ ·2H ₂ O	−1.16	−5.75	−4.58
H ₂ (g)	H ₂	−16.92	−20.02	−3.10
H ₂ O(g)	H ₂ O	−1.79	−0.00	1.79
Halite	NaCl	−8.59	−7.03	1.56
Hausmannite	Mn ₃ O ₄	−35.56	28.11	63.67
Hematite	Fe ₂ O ₃	1.37	−1.82	−3.20
Jarosite-K	KFe(SO ₄) ₂ (OH) ₆	−16.64	−25.03	−8.39
Manganite	MnOOH	−13.16	12.18	25.34
Melanterite	FeSO ₄ ·7H ₂ O	−5.35	−7.69	−2.34
O ₂ (g)	O ₂	−53.05	−55.86	−2.81
Pyrochroite	Mn(OH) ₂	−11.46	3.74	15.20
Pyrolusite	MnO ₂ ·H ₂ O	−22.46	20.62	43.09

References

- Akcil, A.; Koldas, S. Acid Mine Drainage (AMD): Causes, treatment and case studies. *J. Clean. Prod.* **2006**, *14*, 1139–1145. [CrossRef]
- Leiva, E.; Leiva-Aravena, E.; Vargas, I. Acid Water Neutralization Using Microbial Fuel Cells: An Alternative for Acid Mine Drainage Treatment. *Water* **2016**, *8*, 536. [CrossRef]
- Kefeni, K.K.; Msagati, T.A.M.; Mamba, B.B. Acid mine drainage: Prevention, treatment options, and resource recovery: A review. *J. Clean. Prod.* **2017**, *151*, 475–493. [CrossRef]
- Consejo de Monumentos Nacionales de Chile. Fundo Yerba Loca. Available online: <http://www.monumentos.cl/monumentos/santuarios-de-la-naturaleza/fundo-yerba-loc> (accessed on 15 January 2018).
- Ginocchio, R.; Hepp, J.; Bustamante, E.; Silva, Y.; De la Fuente, L.M.; Cásale, J.F.; De la Harpe, J.P.; Urrestarazu, P.; Anic, V.; Montenegro, G. Importance of water quality on plant abundance and diversity in high-alpine meadows of the Yerba Loca Natural Sanctuary at the Andes of north-central Chile. *Rev. Chil. Hist. Nat.* **2008**, *81*, 469–488. [CrossRef]
- Dirección General de Aguas (DGA). *Información Oficial Hidrometeorológica y de Calidad de Aguas en Línea, Reportes Calidad del Agua*; Dirección General de Aguas: Santiago, Chile, 2017. (In Spanish)
- Terry, P.A.; Stone, W. Biosorption of cadmium and copper contaminated water by *Scenedesmus* abundans. *Chemosphere* **2002**, *47*, 249–255. [CrossRef]
- Lockwood, C.L.; Stewart, D.I.; Mortimer, R.J.G.; Mayes, W.M.; Jarvis, A.P.; Gruiz, K.; Burke, I.T. Leaching of copper and nickel in soil-water systems contaminated by bauxite residue (red mud) from Ajka, Hungary: The importance of soil organic matter. *Environ. Sci. Pollut. Res.* **2015**, *22*, 10800–10810. [CrossRef] [PubMed]
- Sipos, P.; Németh, T.; Kis, V.K.; Mohai, I. Sorption of copper, zinc and lead on soil mineral phases. *Chemosphere* **2008**, *73*, 461–469. [CrossRef] [PubMed]
- Slaninova, A.; Machova, J.; Svobodova, Z. Fish kill caused by aluminium and iron contamination in a natural pond used for fish rearing: A case report. *Vet. Med.* **2014**, *59*, 573–581. [CrossRef]
- Ščančar, J.; Stibilj, V.; Milačič, R. Determination of aluminium in Slovenian foodstuffs and its leachability from aluminium-cookware. *Food Chem.* **2004**, *85*, 151–157. [CrossRef]
- Kvech, S.; Edwards, M. Solubility controls on aluminum in drinking water at relatively low and high pH. *Water Res.* **2002**, *36*, 4356–4368. [CrossRef]
- Sorenson, J.R.; Campbell, I.R.; Tepper, L.B.; Lingg, R.D. Aluminum in the environment and human health. *Environ. Health Perspect.* **1974**, *8*, 3–95. [CrossRef] [PubMed]
- Abarca, M.; Guerra, P.; Arce, G.; Montecinos, M.; Escauriaza, C.; Coquery, M.; Pastén, P. Response of suspended sediment particle size distributions to changes in water chemistry at an Andean mountain stream confluence receiving arsenic rich acid drainage. *Hydrol. Process.* **2017**, *31*, 296–307. [CrossRef]

15. Riera, J.; Cánovas, C.R.; Ollás, M. Characterization of main AMD inputs to the Odiel River upper reach (SW Spain). *Procedia Earth Planet. Sci.* **2017**, *17*, 602–605. [[CrossRef](#)]
16. Schemel, L.E.; Kimball, B.A.; Runkel, R.L.; Cox, M.H. Formation of mixed Al–Fe colloidal sorbent and dissolved-colloidal partitioning of Cu and Zn in the Cement Creek—Animas River Confluence, Silverton, Colorado. *Appl. Geochem.* **2007**, *22*, 1467–1484. [[CrossRef](#)]
17. Fuller, C.C.; Davis, J.A. Influence of coupling of sorption and photosynthetic processes on trace element cycles in natural waters. *Nature* **1989**, *340*, 52–54. [[CrossRef](#)]
18. Casiot, C.; Lebrun, S.; Morin, G.; Bruneel, O.; Personne, J.C.; Elbaz-Poulichet, F. Sorption and redox processes controlling arsenic fate and transport in a stream impacted by acid mine drainage. *Sci. Total Environ.* **2005**, *347*, 122–130. [[CrossRef](#)] [[PubMed](#)]
19. Runkel, R.L.; Kimball, B.A. Evaluating remedial alternatives for an acid mine drainage stream: Application of a reactive transport model. *Environ. Sci. Technol.* **2002**, *36*, 1093–1101. [[CrossRef](#)] [[PubMed](#)]
20. Chapman, B.; Jones, D.; Jung, R. Processes controlling metal ion attenuation in acid mine drainage streams. *Geochim. Cosmochim. Acta* **1983**, *47*, 1957–1973. [[CrossRef](#)]
21. Dirección General de Aguas (DGA). *Información Oficial Hidrometeorológica y de Calidad de Aguas en Línea, Reportes Fluviométricos*; Dirección General de Aguas: Santiago, Chile, 2017. (In Spanish)
22. Jirka, A.M.; Carter, M.J. Reactor digestion method. *Anal. Chem.* **1975**, *47*, 1397. [[CrossRef](#)] [[PubMed](#)]
23. Celebi, N.; Nadaroglu, H.; Kalkan, E.; Kotan, R. Removal of copper from copper-contaminated river water and aqueous solutions using *Methylobacterium extorquens* modified Erzurum clayey soil. *Arch. Environ. Prot.* **2016**, *42*, 58–69. [[CrossRef](#)]
24. Sánchez-España, J.; Yusta, I.; Diez-Ercilla, M. Schwertmannite and hydrobasaluminite: A re-evaluation of their solubility and control on the iron and aluminium concentration in acidic pit lakes. *Appl. Geochem.* **2011**, *26*, 1752–1774. [[CrossRef](#)]
25. Ibanez, J.G.; Hernandez-Esparza, M.; Doria-Serrano, C.; Fregoso-Infante, A.; Singh, M.M. Dissolved oxygen in water. In *Environmental Chemistry*; Springer: New York, NY, USA, 2008; pp. 16–27.
26. Chile, NCh 409/2005. *Norma Oficial de Agua Potable*; Instituto Nacional de Normalización: Santiago, Chile, 2005. (In Spanish)
27. Chile, NCh 1.333/1978. *Requisitos de Calidad del Agua para Diferentes Usos*; Instituto Nacional de Normalización: Santiago, Chile, 1978. (In Spanish)
28. Guerra, P.; Gonzalez, C.; Escauriaza, C.; Pizarro, G.; Pasten, P. Incomplete mixing in the fate and transport of arsenic at a river affected by acid drainage. *Water Air Soil Pollut.* **2016**, *227*, 73. [[CrossRef](#)]
29. Nordstrom, D.K.; Ball, J.W. The geochemical behavior of aluminum in acidified surface waters. *Science* **1986**, *232*, 54–56. [[CrossRef](#)] [[PubMed](#)]
30. Nordstrom, D.K.; Alpers, C.N. Geochemistry of acid mine waters. In *The Environmental Geochemistry of Mineral Deposits*; Society of Economic Geologists: Littleton, CO, USA, 1999; pp. 133–160.
31. Nordstrom, D.K. The effect of sulfate on aluminum concentrations in natural waters: Some stability relations in the system $\text{Al}_2\text{O}_3\text{-SO}_3\text{-H}_2\text{O}$ at 298 K. *Geochim. Cosmochim. Acta* **1982**, *46*, 681–692. [[CrossRef](#)]
32. Bertsch, P.M.; Parker, D.R. Aqueous polynuclear aluminum species. *Environ. Chem. Alum.* **1996**, *2*, 117–168.
33. Jones, A.M.; Collins, R.N.; Waite, T.D. Mineral species control of aluminum solubility in sulfate-rich acidic waters. *Geochim. Cosmochim. Acta* **2011**, *75*, 965–977. [[CrossRef](#)]
34. Carrero, S.; Fernandez-Martinez, A.; Pérez-López, R.; Nieto, J.M. Basaluminite structure and its environmental implications. *Procedia Earth Planet. Sci.* **2017**, *17*, 237–240. [[CrossRef](#)]
35. Acero, P.; Ayora, C.; Torrentó, C.; Nieto, J.M. The behavior of trace elements during schwertmannite precipitation and subsequent transformation into goethite and jarosite. *Geochim. Cosmochim. Acta* **2006**, *70*, 4130–4139. [[CrossRef](#)]
36. España, J.S.; Pamo, E.L.; Pastor, E.S.; Andrés, J.R.; Rubí, J.A.M. The removal of dissolved metals by hydroxysulphate precipitates during oxidation and neutralization of acid mine waters, Iberian Pyrite Belt. *Aquat. Geochem.* **2006**, *12*, 269–298. [[CrossRef](#)]
37. De Souza Machado, A.A.; Spencer, K.; Kloas, W.; Toffolon, M.; Zarfl, C. Metal fate and effects in estuaries: A review and conceptual model for better understanding of toxicity. *Sci. Total Environ.* **2016**, *541*, 268–281. [[CrossRef](#)] [[PubMed](#)]
38. Suda, A.; Makino, T. Functional effects of manganese and iron oxides on the dynamics of trace elements in soils with a special focus on arsenic and cadmium: A review. *Geoderma* **2016**, *270*, 68–75. [[CrossRef](#)]

39. Benjamin, M.M.; Leckie, J.O. Multiple-site adsorption of Cd, Cu, Zn, and Pb on amorphous iron oxyhydroxide. *J. Colloid Interface Sci.* **1981**, *79*, 209–221. [[CrossRef](#)]
40. Leiva, E.D.; Rámila, C.D.P.; Vargas, I.T.; Escauriaza, C.R.; Bonilla, C.A.; Pizarro, G.E.; Regan, J.M.; Pasten, P.A. Natural attenuation process via microbial oxidation of arsenic in a high Andean watershed. *Sci. Total Environ.* **2014**, *466–467*, 490–502. [[CrossRef](#)] [[PubMed](#)]
41. Gadde, R.R.; Laitinen, H.A. Heavy metal adsorption by hydrous iron and manganese oxides. *Anal. Chem.* **1974**, *46*, 2022–2026. [[CrossRef](#)]
42. Ociński, D.; Jacukowicz-Sobala, I.; Mazur, P.; Raczyk, J.; Kociotek-Balawejder, E. Water treatment residuals containing iron and manganese oxides for arsenic removal from water—Characterization of physicochemical properties and adsorption studies. *Chem. Eng. J.* **2016**, *294*, 210–221. [[CrossRef](#)]
43. Rajkumar, K.; Ramanathan, A.L.; Behera, P.N. Characterization of clay minerals in the Sundarban mangroves river sediments by SEM/EDS. *J. Geol. Soc. India* **2012**, *80*, 429–434. [[CrossRef](#)]
44. Lee, G.; Bigham, J.M.; Faure, G. Removal of trace metals by coprecipitation with Fe, Al and Mn from natural waters contaminated with acid mine drainage in the Ducktown Mining District, Tennessee. *Appl. Geochem.* **2002**, *17*, 569–581. [[CrossRef](#)]
45. Matichenkov, V.V.; Bocharnikova, E.A. Chapter 13: The relationship between silicon and soil physical and chemical properties. *Stud. Plant Sci.* **2001**, *8*, 209–219. [[CrossRef](#)]
46. Viers, J.; Dupré, B.; Gaillardet, J. Chemical composition of suspended sediments in World Rivers: New insights from a new database. *Sci. Total Environ.* **2009**, *407*, 853–868. [[CrossRef](#)] [[PubMed](#)]
47. Van Breemen, N. *Genesis and Solution Chemistry of Acid Sulfate Soils in Thailand*; Centre for Agricultural Publishing and Documentation: Wageningen, The Netherlands, 1976; ISBN 902200600X.
48. Tait, T. Determination of Copper Speciation, Bioavailability and Toxicity in Saltwater Environments. Master's Thesis, Wilfrid Laurier University, Waterloo, ON, Canada, 2013.
49. McBride, M.B.; Blasiak, J.J. Zinc and copper solubility as a function of pH in an acid soil. *Soil Sci. Soc. Am. J.* **1979**, *43*, 866. [[CrossRef](#)]
50. Elliott, H.A.; Huang, C.P. Adsorption characteristics of some Cu(II) complexes on aluminosilicates. *Water Res.* **1981**, *15*, 849–855. [[CrossRef](#)]



© 2018 by the authors. Licensee MDPI, Basel, Switzerland. This article is an open access article distributed under the terms and conditions of the Creative Commons Attribution (CC BY) license (<http://creativecommons.org/licenses/by/4.0/>).